JOURNAL OF GEOPHYSICAL RESEARCH, VOL. 105, NO. D10, PAGES 12,295–12,302, MAY 27, 2000

Lévy flights and anomalous diffusion in the stratosphere

Kyong-Hwan Seo and Kenneth P. Bowman

Department of Atmospheric Sciences, Texas A&M University, College Station

Abstract. Chaotic transport in the Northern Hemisphere stratosphere is studied with an isentropic Lagrangian transport model. Ensemble statistics of trajectories are computed for 2-month periods in the winters of 1992 to 1997 by using United Kingdom Meteorological Office assimilated winds. In the midlatitudes, quasi-stationary anticyclones combine with the jet to produce flying and trapping events of particle trajectories. The flight time probability density functions (PDFs) are described by power laws with a decay exponent of less than 3, which indicates that the trajectories can be characterized as Lévy flights (random walk processes with divergent second moment). These flight and trapping events lead to superdiffusive zonal dispersion. The relationship between the power law decay exponents and the zonal mean and variance exponents is consistent with an analytical derivation. The scaled PDFs of zonal displacement converge to a self-similar limiting distribution, suggesting the existence of a scale-invariant regime. The skewness and kurtosis of the PDFs also converge to constant values after about 40 days, which supports the self-similarity behavior in Lagrangian trajectories.

1. Introduction

Mixing of long-lived atmospheric trace constituents by the large-scale atmospheric circulation is important for many problems in meteorology and atmospheric chemistry. Among these problems are the formation and disappearance of the springtime Antarctic ozone hole in the stratosphere [*Solomon*, 1990; *Schoeberl and Hartmann*, 1991], the distribution of tropospheric water vapor [*Kelly et al.*, 1991], and the confinement of the aerosols produced by the eruption of Mount Pinatubo to the tropical stratosphere [*Trepte and Hitchman*, 1992; *Minschwaner et al.*, 1996; *Volk et al.*, 1996; *Bowman and Hu*, 1997].

One useful approach to characterizing mixing in fluid flows is the analysis of the separation or dispersion of air parcels, usually represented in theoretical or numerical studies by hypothetical massless air particles that move with the velocity of the flow. Analogies can be made between dispersion in fluid flows and molecular diffusion in a gas. In molecular diffusion, collisions between molecules produce random walks that lead to dispersion of the molecules. In classical molecular diffusion, molecules that are initially located in a compact distribution disperse into a Gaussian distribution whose variance increases linearly with time. The rate of increase of the variance is proportional to the diffusion coefficient for the process. Because the position of a molecule is the result of the sum of a large number of random collisions, the Gaussian behavior follows from the central limit theorem. As long as the statistics of the collisional forcing are reasonably well behaved (i.e., moments are finite), the end result will be Gaussian.

In the case of fluid flows, it is the macroscopic velocity field that leads to dispersion of air particles. In some cases this dispersion resembles molecular diffusion, with particles spreading into a Gaussian distribution with linear time dependence of the variance. The rate of increase of the variance for fluid parcels gives an effective diffusion coefficient (e.g., K_{yy}) that provides one way to characterize mixing in the flow. Effective diffusion coefficients have been helpful in understanding the large-scale structure of mixing behavior and in locating mixing barriers [*Schoeberl et al.*, 1992; *Bowman*, 1993]. *Bowman* [1995] showed that random wave-breaking events in the stratospheric surf zone [*McIntyre and Palmer*, 1983, 1984] can give rise to normal diffusive behavior for air particles in the meridional direction.

There are many examples of fluid flows in which particle dispersion is not Gaussian and the variance does not increase linearly with time. More general forms for the time dependence of the mean and variance are

$$M(t) = \langle \delta x(t) \rangle \propto t^{\beta}, \tag{1a}$$

$$\sigma^2(t) = \left\langle (\delta x(t) - \langle \delta x(t) \rangle)^2 \right\rangle \propto t^{\gamma}, \tag{1b}$$

where $\delta x(t) = x(t) - x(0)$ and angle brackets indicate the average over an ensemble of particles. If the mean particle position grows linearly with time ($\beta = 1$), there is a well-defined transport velocity. If $\beta \neq 1$, however, then the mean transport velocity is either zero or infinite, which is referred to as anomalous advection. In a similar way, in the case of normal diffusion the particle variance σ^2 increases linearly with time ($\gamma = 1$). Anomalous diffusion occurs when $\gamma \neq 1$. Subdiffusive behavior ($0 < \gamma < 1$) occurs when particles are trapped in localized regions or when particles disperse to fill a bounded domain. Superdiffusion ($\gamma > 1$) is caused by long displacements, called "flights", between trapping episodes. For example, ballistic dispersion ($\gamma = 2$) occurs in simple shear flows. If a line of equally spaced particles is initially oriented across a linear shear, the shear will disperse the particles in the along-shear direction by tilting and stretching the line of particles. The length of the line of particles increases linearly with time, while the variance increases quadratically. In all of these cases the dispersion is non-Gaussian and the variance increases nonlinearly because the conditions necessary for the central limit theorem to hold do not apply: either the motion of

Paper number 2000JD900078.
0148-0227/00/2000JD900078$09.00

the particles is not random, or the moments of the forcing do not converge.

One class of random walk processes consists of those with step sizes drawn from a power law distribution $P(\Delta x) \sim \Delta x^{-\eta}$, where $\eta < 3$. The resulting trajectory is called a Lévy flight [*Shlesinger and Klafter*, 1986; *Klafter et al.*, 1987; *Solomon et al.*, 1993, 1994; *Klafter et al.*, 1996; *Weeks et al.*, 1996; *del-Castillo-Negrete*, 1998]. Lévy flights can be characterized by the probability density functions (PDFs) of their step size or, equivalently, assuming constant velocities, by the PDFs of their flight times. In the case of variable flight speeds, differences in the slope between the flight step size and time PDFs are likely small as long as flights occur in the finite band of the jet stream. For Lévy flights the second moment of the step size PDF in the generalized random walk goes to infinity; so the central limit theorem does not apply. In addition to nonlinearly increasing variance with time, Lévy flights have non-Gaussian particle distributions. Simple ballistic motion is a special case of a Lévy flight. Figure 1 illustrates the difference between normal diffusion and Lévy flights with a simple analytical stochastic model. Each trajectory consists of a series of steps drawn from a power law distribution of step sizes. For the normal random walk (Figure 1a), η is greater than 3, and large displacements are extremely rare. For the Lévy flights (Figure 1b), η is 0.89, and the motion has a number of large jumps between many small displacements. The long steps dominate the overall motion.

The behavior of Lévy flights has been classified for symmetric and asymmetric random walks by *Weeks et al.* [1996]. Lévy flights and superdiffusion of passive tracer particles have been observed in a flow composed of a series of quasi-steady vortices in a rapidly rotating annulus [*Solomon et al.*, 1993, 1994; *Weeks et al.*, 1996]. In the rotating tank experiments the flight time and trapping time PDFs exhibit power law behavior. In the atmosphere, *Pierrehumbert and Yang* [1993] found ballistic zonal tracer dispersion ($\gamma \approx 2$) in the upper troposphere using isentropic trajectories from a general circulation model.

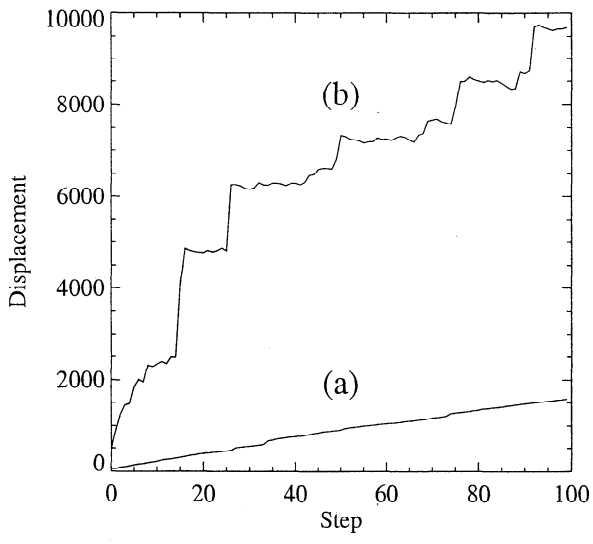

Figure 1. (a) Random walk process leading to normal diffusion for 100 steps and (b) random walk process (Lévy flights) leading to superdiffusive dispersion for 100 steps. For both random walks, the mean step size is the same. The step length is drawn from a power law PDF, $P(\Delta x) \sim \Delta x^{-\eta}$ with (a) $\eta = 3.5$, and (b) $\eta = 0.89$. The case of Figure 1b uses a value of $\eta = 0.89$ drawn from the observed statistics (see section 3.1). Note that in Figure 1b the motion consists of a series of flight and trapping events.

Anomalous diffusion and non-Gaussian dispersion of passive tracers has also been studied in idealized analytical flows. For a large-amplitude single-frequency traveling wave perturbed by a wave with a second frequency, tracer particles exhibit chaotic advection and superdiffusive behavior in the chaotic separatrix layer or stochastic layer, which lies between the trapped and free regions of the flow [*Weiss and Knobloch*, 1989; *Weiss*, 1991]. The mechanisms of asymmetric transport and the departures from Gaussian behavior in the statistics of passive scalars within the stochastic layer in a chain of vortices in a shear layer were investigated by *del-Castillo-Negrete* [1998] by using an analytical model with the regular neutral modes of the quasi-geostrophic equation and a discrete map model. Because of the asymmetries in the flow, mixing between the vortices and the upstream flow was different from mixing between the vortices and downstream flow. He showed that anomalous advection and anomalous diffusion occur, and the flight PDFs correspond to Lévy flights in the layer due to the coherent structures such as the vortices and shear flow.

Here we investigate whether Lévy flights, anomalous diffusion, and non-Gaussian dispersion can be found in large-scale atmospheric flows, and we discuss the physical mechanism for anomalous diffusion. We present 6-year ensemble statistics of the moments and flight and trapping PDFs for the wintertime Northern Hemisphere stratosphere by using observed atmospheric wind fields. The Northern Hemisphere middle and upper stratosphere are characterized by large-amplitude quasi-stationary features, principally the Aleutian anticyclone. Variations in the strength of the Aleutian anticyclone lead to flying and trapping events. The relationship between anomalous diffusion and the power law PDFs of the flight and trapping times is compared with the prediction from a continuous time random walk (CTRW) model [*Weeks et al.*, 1996; see also *Klafter et al.*, 1987].

2. Model and Data

2.1. Lagrangian Trajectory Model

A Lagrangian trajectory model is used to calculate the trajectories of idealized massless particles on isentropic surfaces. Particle positions are integrated by using a standard fourth-order Runge-Kutta scheme and United Kingdom Meteorological Office (UKMO) assimilated winds (see below). Trajectories are limited to 2 months to avoid nonstationary effects from the seasonal cycle. The Lagrangian equations of motion in spherical coordinates are

$$\frac{d\lambda}{dt} = \frac{u(\lambda,\phi,t)}{a\ cos\ \phi},$$
$$\frac{d\phi}{dt} = \frac{v(\lambda,\phi,t)}{a}, \qquad (2)$$

where λ and ϕ denote longitude and latitude, respectively, and a is the radius of the Earth. Velocities are interpolated linearly in space and time from gridded data to the particle locations. A detailed description of the model can be found in the work of *Bowman* [1993]. Calculations show that parcels initialized north of 50°N or south of 30°N typically remain inside the vortex or in the subtropics, respectively, and do not alternate between trapping and flight. Therefore trajectories are calculated for 120×30 arrays of particles initially arranged in a regular

longitude-latitude grid extending from 30°N to 50°N. This excludes a small number of parcels that might undergo flying and trapping events. For particle dispersion statistics in the longitudinal direction, the position of each particle is tracked as though longitude extends to $\pm\infty$, although the flow is periodic with period 360°. When particles cross the Greenwich meridian, their longitude is not folded into the range 0°–360° but is allowed to increase or decrease indefinitely.

2.2. UKMO Analyses

The wind fields used as input to the trajectory model come from the stratospheric version of the data assimilation system used at the United Kingdom Meteorological Office for operational weather forecasting [*Lorenc et al.*, 1991; *Swinbank and O'Neill*, 1994]. Stratospheric fields are derived primarily from the TIROS-N series of polar-orbiting satellites operated by the National Oceanic and Atmospheric Administration and from radiosonde soundings. Additional observations comprise aircraft winds and temperatures, satellite cloud track winds, and surface observations of pressures. The analyzed three-dimensional global fields of temperature, geopotential height, and winds are stored once per day on a global 3.75° × 2.5° longitude-latitude grid at 22 Upper Atmosphere Research Satellite pressure levels extending from 1000 to 0.316 hPa (surface to mesosphere). Winds are interpolated linearly in log θ onto isentropic surfaces for use in the Lagrangian trajectory model.

3. Results

3.1. Lévy Flights in the Northern Hemisphere

The wintertime Northern Hemisphere middle and upper stratosphere has large quasi-stationary anticyclones: the Aleutian and Atlantic anticyclones [*Harvey and Hitchman*, 1996]. Fluctuations in the amplitude or position of these vortices offer the possibility of intermittently trapping particles within the anticyclones, leading to Lévy flights. We examine trajectories on the 850 K isentropic surface (~10 hPa in midlatitudes) for January and February of 1992, 1994, 1995, 1996, and 1997 and February and March of 1993. We choose these periods to ensure that the Aleutian anticyclone persists throughout the period at this level. Because the anticyclone in 1993 vanished after January 13 and redeveloped at the end of the month, this month is excluded.

Figure 2 shows representative maps of the Montgomery stream function fields at 850 K for each individual year. All maps have the stratospheric extension of the Aleutian high near the date line. The Aleutian high originally develops over the western Pacific in the troposphere. In some years, another anticyclone appears over the Atlantic (e.g., 1994 and 1996). While the anticyclones strengthen and weaken during the 2 months, the positions of their centers are nearly stationary. Along with these two anticyclones, a well-organized polar vortex is seen. The jet is located along the outer boundary of the polar vortex.

To illustrate the character of parcel motion during this period, three particle trajectories in each year are plotted in Figure 3. The trapping regions are clearly identified: one over the Pacific and, in some cases, one over the Atlantic. The horizontal size of the trapping loop is associated with the amplitude and strength of each vortex. Figure 4 shows zonal displacements for the three individual parcels corresponding to the trajectories in Figure 3. Flights are periods when the longitudes of parcels increase for extended periods. The rate of increase is approximately given by the speed of the jet. During trapping events, parcel longitudes generally oscillate within a restricted range as the parcels circulate around the anticyclones. As can be seen, particles typically alternate between moving around the polar vortex and being trapped in the anticyclones. The flight speeds for different particles are similar but not identical owing to the nonconstant wind speed near the jet.

Since particles travel long distances for random lengths of times in the jets and are stuck for random intervals of time in the vortices, we compute the probability distribution functions. To calculate PDFs for flight and trapping times, we define a step as a monotonic zonal displacement between reversals of direction. A flight, then, is a step larger than the approximate size of the anticyclones, $\Delta\lambda$, chosen here to be 90°. Trapping occurs when the trajectory reverses before moving the zonal distance $\Delta\lambda$. Testing shows that the PDFs of flight and trapping events are not sensitive to appreciable changes in $\Delta\lambda$. Only those particles experiencing both flight and trapping episodes are considered in the calculation of variance and PDFs. This excludes 15–40% of total particles, depending on year. This criterion may eliminate from the statistics some parcels undergoing very long flying or trapping events. It also eliminates many particles that would never experience a transition between trapping in the vortices and flying in the jet during a single season. The last step of each trajectory is excluded in calculation since its flight or trapping time is undetermined by this finite integration time. Figure 5 shows the ensemble flight and trapping time PDFs for the selected particles. We can see that both the flight and trapping PDFs can be described by power law scaling, $P_f(t) \propto t^{-\mu}$ and $P_t(t) \propto t^{-\nu}$. Because the slopes of the power law relationships, (μ=1.12 and ν=1.08), are less than 3, the trajectories can be characterized as Lévy flights.

Figure 6 shows the flight length PDF, which also exhibits algebraic decay: $P_{fl}(\Delta x) \propto \Delta x^{-\eta}$ with the decay exponent η = 0.89. This differs from the flight time PDF by ~20%. The difference represents the variability in flight speed, which depends upon time and location. A random walk behavior using the observed flight and trapping length statistics is shown in Figure 1b for 100 steps. The several long steps induce the slow decay of the power law approximation. While a characteristic size of the normal random walks (Figure 1a) is expressed as a square root of the mean square displacement, the random walks of Lévy flights have no characteristic length.

Trajectories with Lévy flights usually lead to anomalous diffusion. Figure 7 shows the evolution of the zonal mean and variance for the selected particles between 30° and 50°N. Since the mean particle position, $M(t)$, grows approximately linearly in time (β = 1.05), the trajectories do not exhibit anomalous advection. In this case, the mean transport velocity, expressed as $V = \lim_{t\to\infty} (M/t)$, can be well defined. On the other hand, the rate of growth of the variance is significantly larger than linear, displaying superdiffusive dispersion. The subballistic motion comes from the fact that zonal transport of parcels is somewhat suppressed by trapping in the anticyclones. If there were no trapping mechanism, then ballistic motion (γ = 2) would appear.

The relationship between μ, ν, β, and γ is roughly consistent with the analytical model of *Weeks et al.* [1996] (their Figure 1 and Tables 2 and 3). For an asymmetric random walk with a constant velocity

$$\beta = 1 + \nu - \mu \quad 1 < \mu < 2 \text{ and } 1 < \nu < \mu; \tag{3a}$$

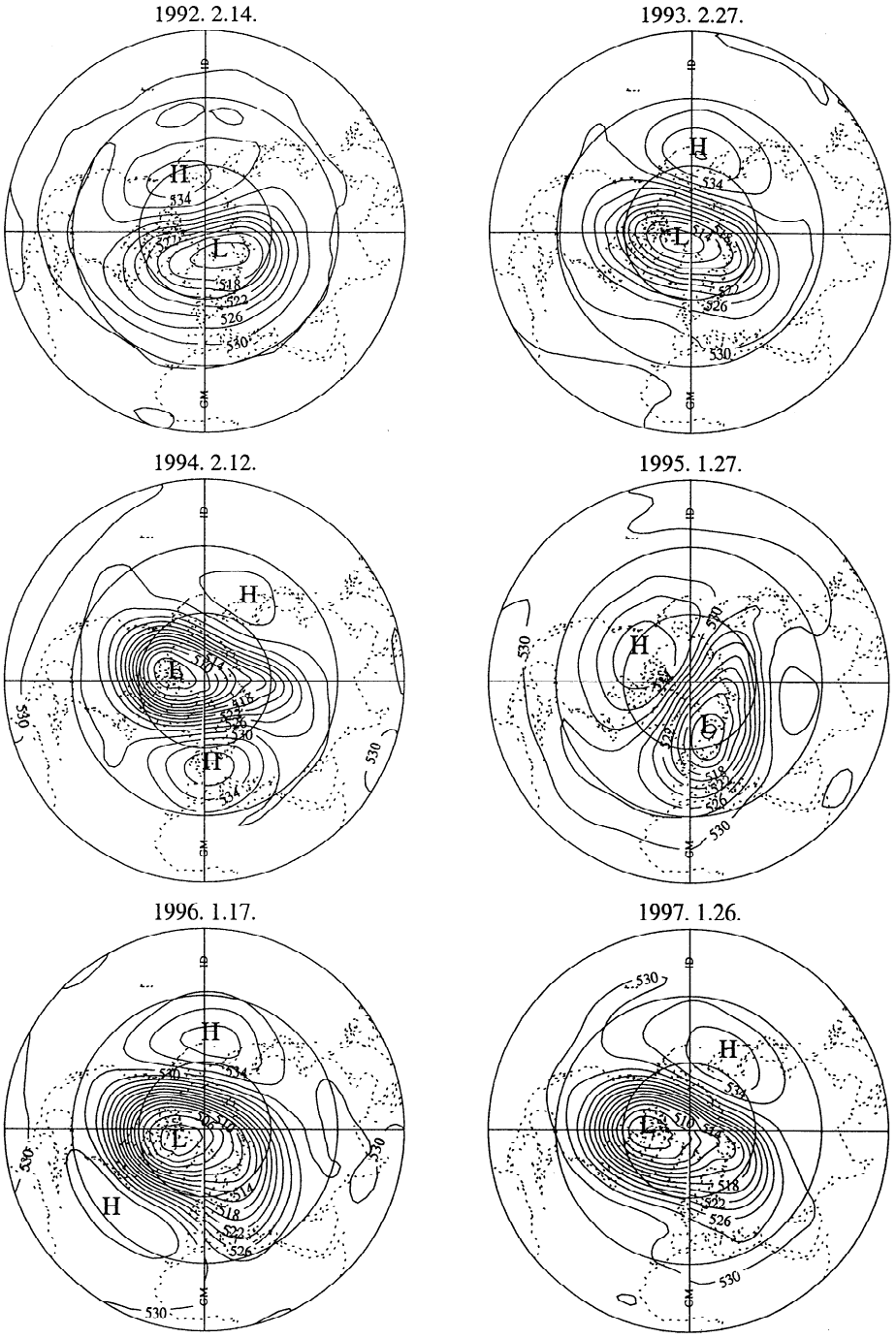

Figure 2. Montgomery stream functions (×1000 m^2s^{-2}) in the Northern Hemisphere at 850 K at 1200 UTC for each year.

$$\gamma = 2 + \nu - \mu \quad \nu < \mu < 4 - \nu \text{ and } 1 < \nu < 2. \qquad (3b)$$

The value of β estimated from μ and ν by using (3a), 0.96, is compared with the calculated value of 1.05. The values of γ calculated from (3b) and (1b) are 1.96 and 1.86, respectively. Once again, the small differences likely arise from nonconstant flight speeds associated with the jet, which are not taken into account in (3).

3.2. Self-Similar Scaling

In order to see a scale invariant dispersion with relation to Lévy flights, the time evolution of the PDFs is calculated by introducing the scaling parameter, $t^{\gamma/2}$, where γ is taken from Figure 7. Figure 8 shows scaled PDFs, $t^{\gamma/2}P(X,t)$ as a function of the scaling variable $\eta = Xt^{\gamma/2}$ at 10-day intervals for 2 months. The variable X is defined as $X = \delta x - \langle \delta x \rangle$. We can see that an asymmetric distribution is evident at all times and the PDFs have a peculiar multimodal shape due to the fairly long particle movement along the jets. The PDFs approach a limiting distribution at successive times after ~40 days of particle dispersion. That is, the distribution curves collapse into a self-similar distribution of the form

$$P(X,t) = t^{-\gamma/2} f\left(\frac{X}{t^{\gamma/2}}\right), \qquad (4)$$

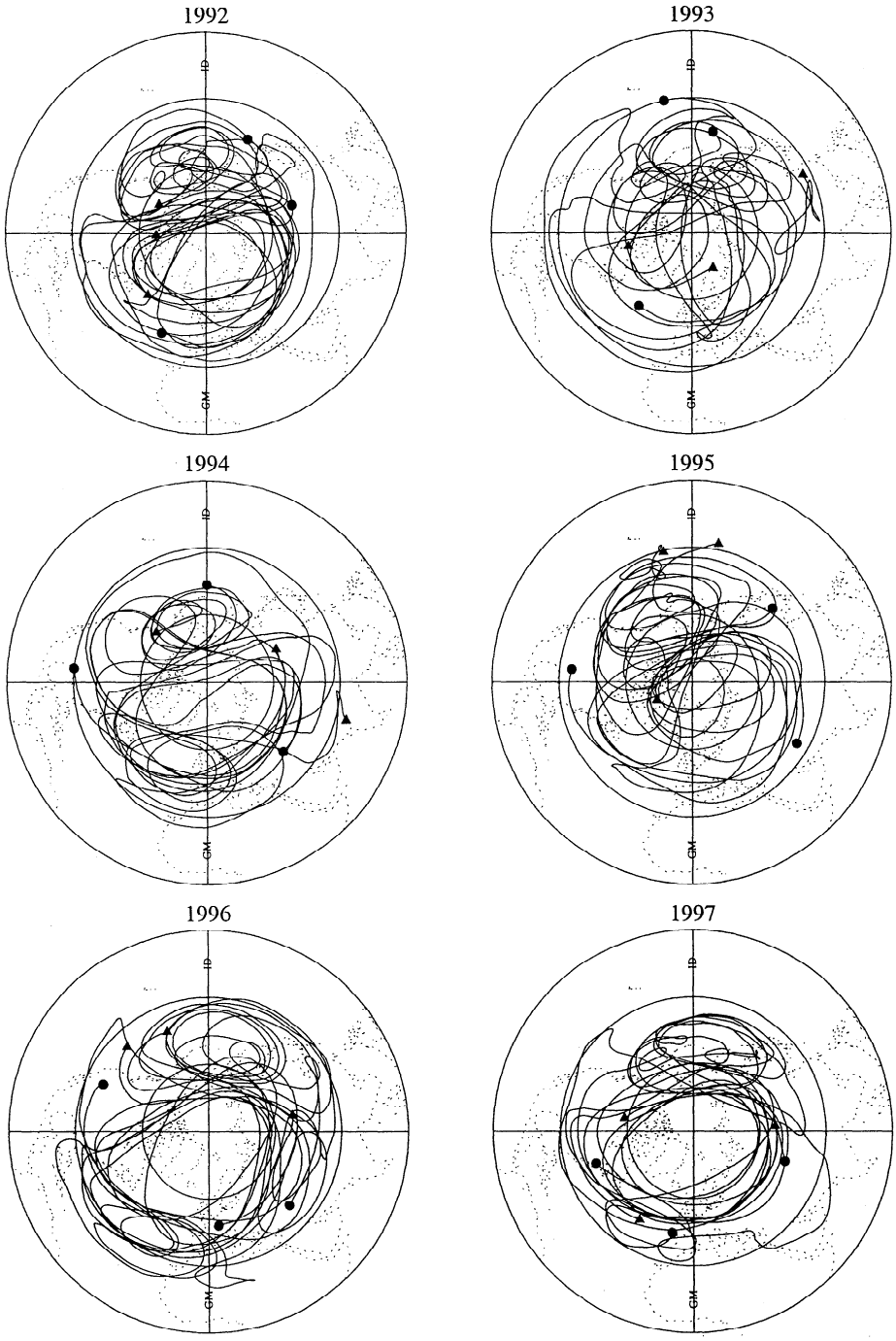

Figure 3. Composite plot of three individual parcel trajectories for 2 months for each year. The initial position of each trajectory is marked by a circle; the final position by a triangle.

where f is any scaling function. This property is physically or statistically anticipated from the characteristics of Lévy flights, since the particle trajectories show self-similar appearance and are composed of fractal structure [e.g., *Shlesinger and Klafter*, 1986; *Klafter et al.*, 1996]. This is, thus, invariant under the space and time rescaling [*del-Castillo-Negrete*, 1998].

The convergence of the distribution to a self-similar form suggests that as time goes to infinity, all moments of the distribution scale as

$$\langle X^n \rangle \propto t^{nr/2}, \tag{5}$$

through the relationship

$$\langle X^n \rangle = \int X^n P(X,t) dX . \tag{6}$$

Note that when γ equals 1, the moments are Gaussian. The scaling law for the moment, (5), also implies that the skewness and kurtosis, which correspond to the normalized third and fourth moment, respectively, defined as

$$S = \frac{\langle X^3 \rangle}{\sigma^3}, \quad K = \frac{\langle X^4 \rangle}{\sigma^4}, \tag{7}$$

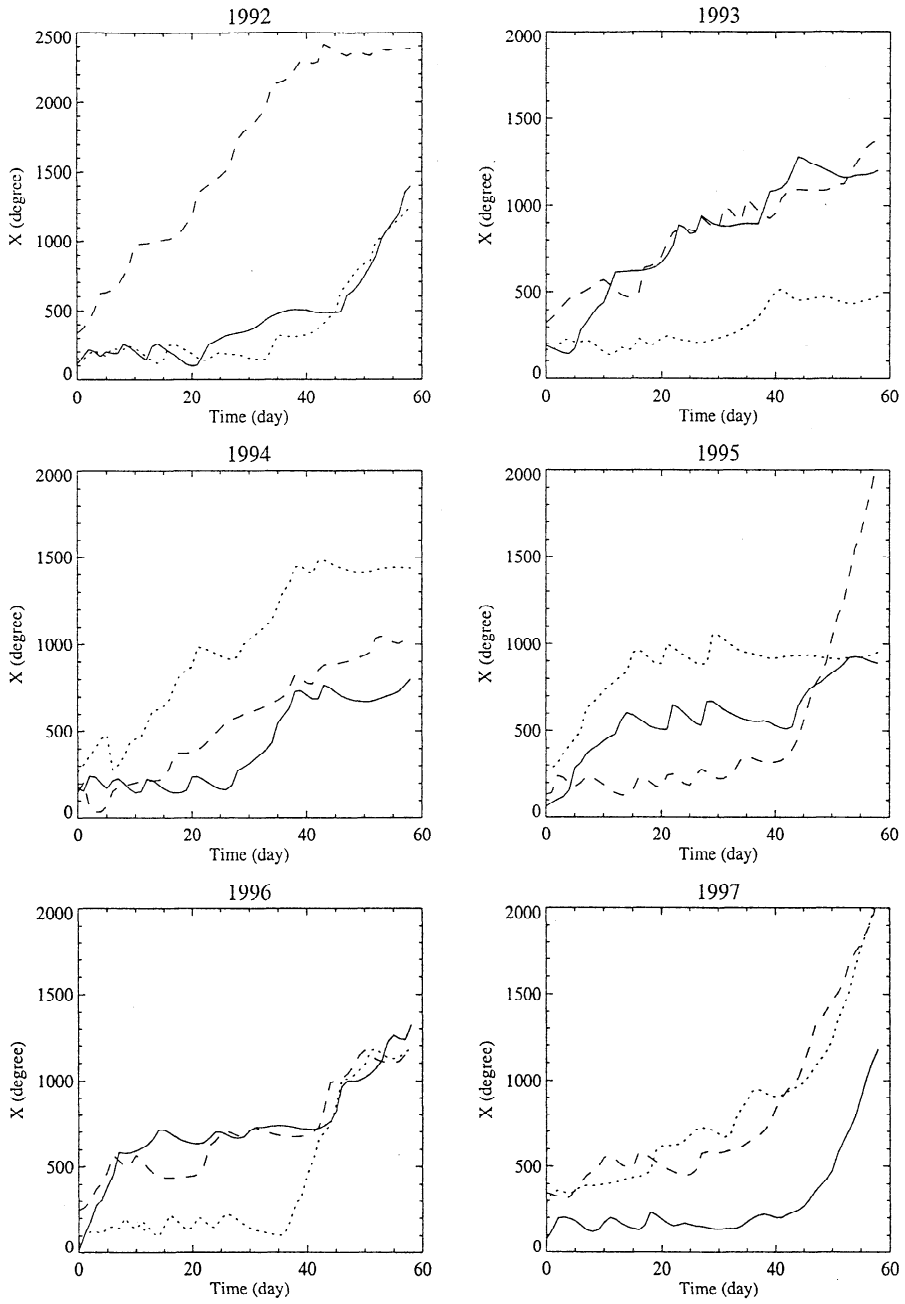

Figure 4. Zonal displacements over 2 months for the three parcels in Figure 3. The initial position of each parcel is chosen arbitrarily for clarity.

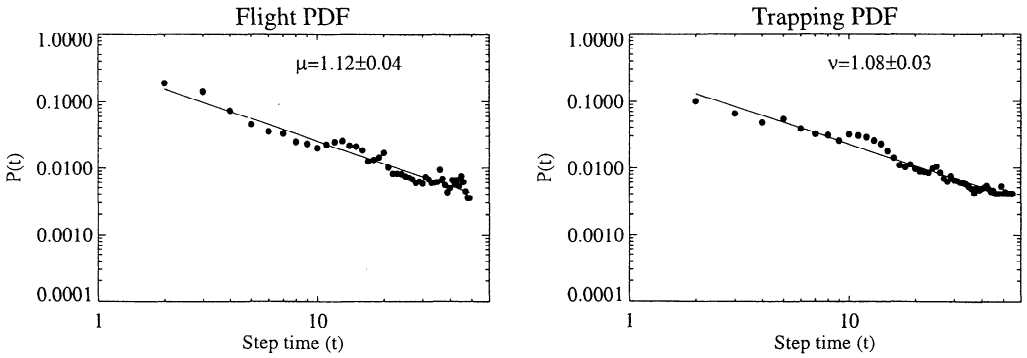

Figure 5. Ensemble average flight and trapping time PDFs. The values of the decay exponents from power law approximation are included in the plots.

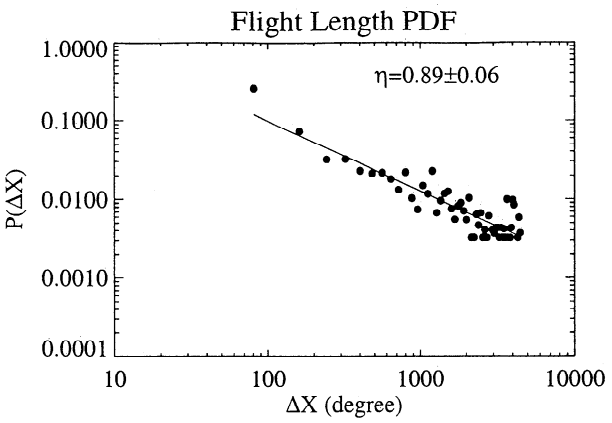

Figure 6. Ensemble average flight length PDF. The value of the decay exponent from power law approximation is included in the plot.

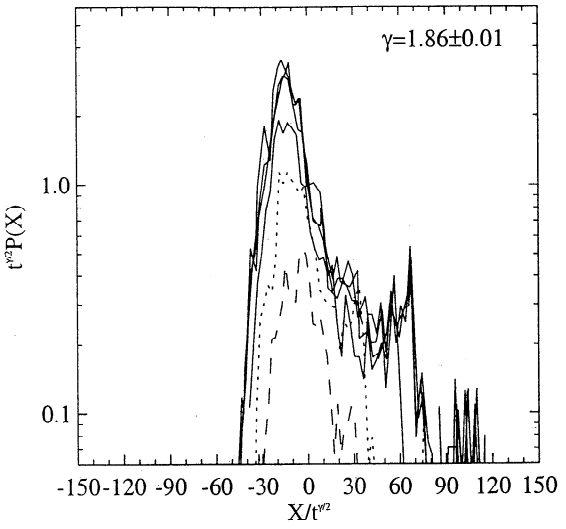

Figure 8. Scaled PDFs of particle displacements, $t^{\gamma/2}P(X,t)$, as a function of scaling variable $\eta = Xt^{\gamma/2}$ at intervals of 10 days for 2 months starting from January 9 (dashed line).

should be constant at large times [*del-Castillo-Negrete*, 1998]. Skewness is a measure of a lack of symmetry in a probability distribution, and kurtosis is a measure of how fat a probability distribution's tails are or a measure of peakedness in the center of a probability distribution. For the normal distribution, $S = 0$ and $K = 3$. As is shown in Figure 9, the distribution is positively skewed, and the tails of the probability distribution are thicker than those of a corresponding normal distribution. More importantly, these normalized moments all tend to converge after 40 days. This convergence is another means of checking for the existence of a self-similar probability distribution and, hence, supports the idea that the selected trajectories have a self-similar nature.

4. Summary and Conclusions

Chaotic advection in the stratosphere is studied by computing the dispersion statistics of Lagrangian particles transported by observed winds. In the Northern Hemisphere, the anticyclones and the jet stream form a favorable environment for inducing Lévy flights and chaotic transport. Particle trajectories in the stochastic layer show alternating flight and trapping episodes. The PDFs of flight and trapping times exhibit power law decay with an exponent of less than 3, indicating that the trajectories can be characterized as Lévy flights. This result is the first analysis to show Lévy flight behavior in large-scale geophysical flows. The ensemble particle dispersion grows as a power law with time and appears superdiffusive. Reasonably good agreement is found between direct calculation of dispersion statistics and estimates made from time PDFs by using CTRW theory. Differences between theory and observations can be attributed to the nonconstant velocities in the observed flow. The displacement PDFs have a multimodal non-Gaussian distribution due to particles traveling long distances in the jet.

The scaled PDFs approach a limiting distribution at successive times after 40 days of particle dispersion in the Northern Hemisphere. This collapse to a self-similar curve strongly implies that the particle trajectories behave as Lévy flights and supports the existence of a scale invariant regime. Also the saturation of the skewness and kurtosis helps to verify the convergence to a self-similar probability distribution. Thus as long as coherent structures persist, the statistical behavior of particle dispersion can be estimated. The divergent second moments of the length PDFs result in the absence of a characteristic length scale for random walks.

Anomalous diffusion is related to the slow algebraic decay of the Lagrangian velocity autocorrelation function $R_L = \langle u(t)u(t+\tau)\rangle$ with lag τ [*McComb*, 1991; see also *del-Castillo-Negrete*, 1998] compared with the normal diffusion case. That is, the important factor in producing anomalous diffusion and non-Gaussian distribution of particle displacement is long-time correlations in the Lagrangian velocity. In the case of

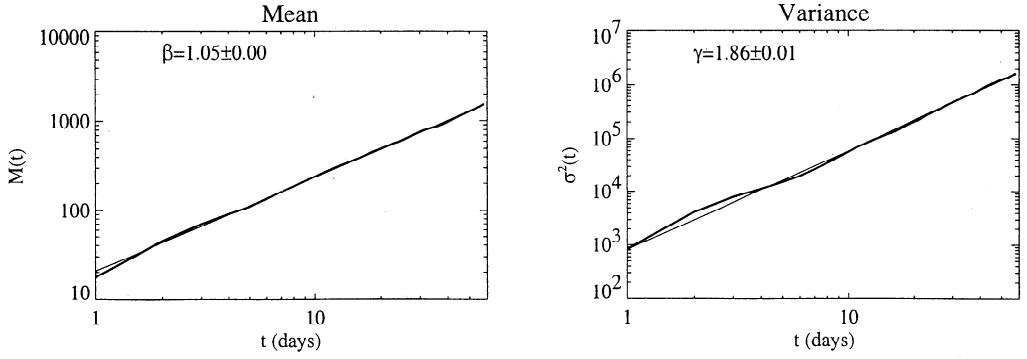

Figure 7. Time evolution of the zonal mean, $M(t)$, and variance, $\sigma^2(t)$. The error is the ensemble standard deviation.

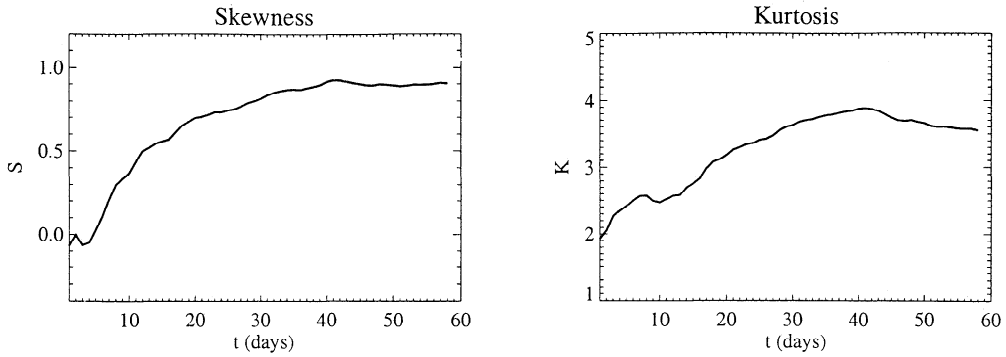

Figure 9. Skewness and kurtosis as a function of time.

turbulent or weakly turbulent flow [*Solomon et al.*, 1993, 1994], R_L decays sufficiently quickly with time to produce normal diffusion with an exponential PDF. For the Northern hemisphere Lévy flights cases, the long-time correlation is caused by the coherent structures: the anticyclone(s) and the jet.

Acknowledgments. We would like to thank Diego del-Castillo-Negrete at Los Alamos National Laboratory for valuable discussions on the self-similar scaling problems. We also appreciate the helpful comments on dispersion in the stratosphere by Lynn Sparling. The comments of an anonymous reviewer are gratefully acknowledged. This work was funded by NASA grants NAG-1-1896 and NAG5-6481.

References

Bowman, K. P., Large-scale isentropic mixing properties of the Antarctic polar vortex from analyzed winds, *J. Geophys. Res.*, *98*, 23,013-23,027, 1993.

Bowman, K. P., Diffusive transport by breaking waves, *J. Atmos. Sci.*, *52*, 2416-2427, 1995.

Bowman, K. P., and Y. Hu, Tropical mixing barrier in the lower stratosphere in the Geophysical Fluid Dynamics Laboratory SKYHI model, *J. Geophys. Res.*, *102*, 21,465-21,478, 1997.

del-Castillo-Negrete, D., Asymmetric transport and non-Gaussian statistics of passive scalars in vortices in shear, *Phys. Fluids*, *10*, 576-594, 1998.

Harvey, V. L., and M. H. Hitchman, A climatology of the Aleutian high, *J. Atmos. Sci.*, *53*, 2088-2101, 1996.

Kelly, K. K., A. F. Tuck, and T. Davies, Wintertime asymmetry of upper tropospheric water between the Northern and Southern Hemisphere, *Nature*, *353*, 244-247, 1991.

Klafter, J., A. Blumen, and M. F. Shlesinger, Stochastic pathway to anomalous diffusion, *Phys. Rev. A*, *35*, 3081-3085, 1987.

Klafter, J., M. F. Shlesinger, and G. Zumofen, Beyond Brownian motion, *Phys. Today*, *49*, 33-39, 1996.

Lorenc, A. C., R. S. Bell, and B. MacPherson, The Meteorological Office analysis correction data assimilation scheme, *Q. J. R. Meteorol. Soc.*, *117*, 59-89, 1991.

McComb, W. D., *The Physics of Fluid Turbulence*, pp. 437-441, Oxford Univ. Press, New York, 1991.

McIntyre, M. E., and T. N. Palmer, Breaking planetary waves in the stratosphere, *Nature*, *305*, 593-600, 1983.

McIntyre, M. E., and T. N. Palmer, The "surf zone" in the stratosphere, *J. Atmos. Terr. Phys.*, *46*, 825-849, 1984.

Minschwaner, K., A. E. Dessler, J. W. Elkins, C. M. Volk, D. W. Fahey, M. Loewenstein, J. R. Podolske, A. E. Roche, and K. R. Chan, Bulk properties of isentropic mixing into the tropics in the lower stratosphere, *J. Geophys. Res.*, *101*, 9433-9436, 1996.

Pierrehumbert, R. T., and H. Yang, Global chaotic mixing on isentropic surfaces, *J. Atmos. Sci.*, *50*, 2462-2480, 1993.

Schoeberl, M. R., and D. L. Hartmann, The dynamics of the stratospheric polar vortex and its relation to springtime ozone depletion, *Science*, *251*, 46-52, 1991.

Schoeberl, M. R., L. R. Lait, P. A. Newman, and J. E. Rosenfield, The structure of the polar vortex, *J. Geophys. Res.*, *97*, 7859-7882, 1992.

Shlesinger, M. F., and J. Klafter, Lévy walk representations of dynamics processes, in *Perspectives in Nonlinear Dynamics*, edited by M. F. Shlesinger, R. Cawley, A. W. Saenz, and W. Zachary, pp. 336-349, World Sci., River Edge, N. J., 1986.

Solomon, S., Progress towards a quantitative understanding of Antarctic ozone depletion, *Nature*, *347*, 347-354, 1990.

Solomon, T. H., E. R. Weeks, and H. L. Swinney, Observations of anomalous diffusion and Lévy flights in a two-dimensional rotating flow, *Phys. Rev. Lett.*, *71*, 3975-3978, 1993.

Solomon, T. H., E. R. Weeks, and H. L. Swinney, Chaotic advection in a two-dimensional flow: Lévy flights and anomalous diffusion, *Physica D*, *76*, 70-84, 1994.

Swinbank, R., and A. O'Neill, A stratosphere-troposphere data assimilation system, *Mon. Weather Rev.*, *122*, 686-702, 1994.

Trepte, C. R., and M. H. Hitchman, Tropical stratospheric circulation deduced from satellite aerosol data, *Nature*, *355*, 626-628, 1992.

Volk, C. M., J. W. Elkins, D. W. Fahey, R. J. Salawitch, G. S. Dutton, J. M. Gilligan, M. H. Profitt, M. Loewenstein, J. R. Podolske, K. Minschwaner, J. J. Margitan, and K. R. Chan, Quantifying transport between the tropical and mid-latitude lower stratosphere, *Science*, *272*, 1763-1768, 1996.

Weeks, E. R., J. S. Urbach, and H. L. Swinney, Anomalous diffusion in asymmetric random walks with a quasi-geostrophic flow example, *Physica D*, *97*, 291-310, 1996.

Weiss, J. B., Transport and mixing in traveling waves, *Phys. Fluids A*, *3*, 1379-1384, 1991.

Weiss, J. B., and E. Knobloch, Mass transport and mixing by modulated traveling waves, *Phys. Rev. A*, *40*, 2579-2589, 1989.

K. P. Bowman, and K.-H. Seo, Department of Atmospheric Sciences, Texas A&M University, College Station, TX 77843-3150. (k-bowman@tamu.edu; khseo@csrp.tamu.edu)

(Received May 13, 1999; revised October 22, 1999; accepted December 13, 1999.)